Full-Duplex Multiuser Wireless Information and Power Transfer With a Multistage Nonlinear Rectifier Energy Harvesting Model

Derek Kwaku Pobi Asiedu, Ji-Hoon Yun

Full-Duplex Multiuser Wireless Information and Power Transfer with a Multistage Nonlinear Rectifier Energy Harvesting Model

Derek Kwaku Pobi Asiedu, *Member, IEEE*, and Ji-Hoon Yun, *Senior Member, IEEE*

***Abstract*—This work investigates radio resource allocation for simultaneous wireless information and power transfer between a full-duplex (FD) multiantenna access point (AP) and multiple half-duplex (HD) single-antenna energy harvesting (EH) user equipment devices (UEs). The EH model of an advanced multistage rectifier circuit design is derived and used for radio resource allocation. To account for both downlink (DL) and uplink (UL) traffic for each of the HD UEs, alternating DL and UL communication phases between two UE groups are considered. We use the weighted minimum mean squared error approach to develop an iterative algorithm to maximize the system sum rate, utilizing optimal receive and transmit beamformers.**

***Index Terms*—energy harvesting, simultaneous wireless information and power transfer, full-duplex communication**

I. Introduction

The advantage of a single-channel full-duplex (FD) system over a half-duplex (HD) system is its potential to double the achievable rate [1]. Recently, attempts have been made to combine FD systems with energy harvesting (EH) technology. EH is the process of scavenging energy from radio frequency (RF) signals to power or recharge the batteries of communication devices. An EH FD system facilitates simultaneous wireless information and power transfer (SWIPT) [2], using the time switching method and/or the power splitting ratio (PSR) method.

EH circuit design greatly affects EH performance and, thus, system optimization. After the development of a new EH circuit design, the formulation of its mathematical model follows, enabling its integration into system optimization processes. Several mathematical models of EH circuitry have been proposed, which can be grouped into linear EH (L-EH) [3] and nonlinear EH (NL-EH) models [2], [4], [5], [6]. L-EH models are deficient in accurately capturing the influence of the EH circuit (i.e., antenna and rectifier circuit) on the RF signal behavior and the amount of energy harvested. Meanwhile, threshold- and sigmoid-based NL-EH models [2], [4], [6] also fail to represent actual EH circuit implementations since necessary threshold and experimental values are specific to a particular EH circuit design or device [4], [5]. Recently, an EH rectifier model was proposed in [5] that could more closely approximate actual EH circuit behavior. In the meantime, EH rectifier circuit development has further evolved toward the use of a multistage rectifier to enhance EH efficiency, as shown in [7] by overcoming the nonlinearity of Schottky barrier diodes, which presents the circuit design that is currently the best available in practice.

EH FD-SWIPT system optimization has been studied in [3], [4], [6], [8], considering either energy minimization or rate maximization. However, none of the existing works has considered single-/multistage EH rectifier models. Moreover, in general, users have both downlink (DL) and uplink (UL) traffic requirements. If user equipment devices (UEs) are capable only of HD operation (due to the costs and complexity of self-interference (SI) cancellation), then the FD access points (APs) still need to serve each UE with both DL and UL communication in different time slots. Existing studies on FD/HD-SWIPT systems, however, have either considered users dedicated to either DL or UL communication only or have separated EH users [3], [4], [6], [8].

This paper investigates a multiuser EH FD-SWIPT system using a newly derived multistage rectifier EH model. To account for both DL and UL traffic for each of the HD UEs, alternating DL and UL communication phases with adjustable durations between two UE groups is considered. First, we derive the output voltage and harvested power for the multistage rectifier EH circuit model. This model is parameterized with a versatile set of design parameters, allowing it to adapt to a wide range of operational environments. Then, the PSR, time slot durations, transmit and receive beamformers, and UE grouping are derived to maximize the DL and UL sum rate under power budget constraints. We use the weighted minimum mean squared error (WMMSE) approach [9] to develop an iterative algorithm to achieve the suboptimal system objective of maximizing the sum-rate. Simulation results demonstrate that the proposed radio resource allocation scheme in conjunction with the advanced EH model significantly outperforms benchmark schemes with conventional EH models.

Notations: $\mathbf{A} \in \mathbb{C}^{M\times N}$ is a matrix with dimensions of M by N. $\mathbf{a} \in \mathbb{C}^{M\times 1}$ is a vector with dimensions of M by 1. a is a scalar variable. $\mathbf{I}_M$ represents the identity matrix with dimensions of M by M. $z \sim \mathcal{CN}(0, \sigma^2)$ denotes a circularly symmetric Gaussian random variable with zero mean and a variance of σ^2. A superscript H on a variable indicates the Hermitian transpose of that variable. $x^\star$ is the optimal value of the variable x for a given problem.

II. System Model, EH Model and Problem Formulation

An FD AP with $2M$ antennas communicating with K single-antenna HD UEs is considered in this paper. The FD AP uses M antennas for DL communication and the other M antennas for UL communication. The UEs are divided into two groups,

Derek Kwaku Pobi Asiedu and Ji-Hoon Yun are with the Department of Electrical and Information Engineering, Seoul National University of Science and Technology, Seoul 01811, Republic of Korea.

Corresponding author: Ji-Hoon Yun (email: jhyun@seoultech.ac.kr).

This study was financially supported in part by the Basic Science Research Program through the National Research Foundation of Korea (NRF) funded by the Ministry of Education under Grant NRF-2019R1A6A1A03032119 and in part by Seoul National University of Science and Technology.

This article has been accepted for publication in IEEE Wireless Communications Letters. This is the author's version which has not been fully edited and content may change prior to final publication. Citation information: DOI 10.1109/LWC.2023.3324984

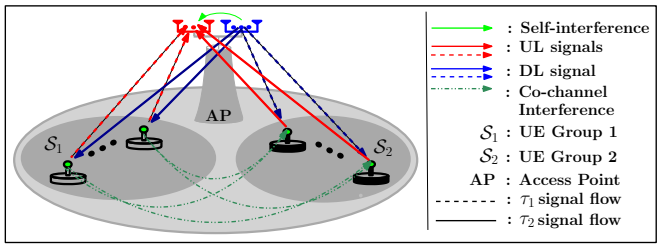

Fig. 1. Proposed multiuser FD-SWIPT system model.

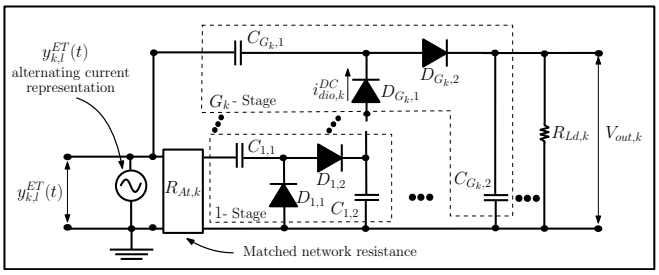

Fig. 2. G_k-stage EH circuit diagram.

alternating between DL and UL communications in distinct time slots. The first group, $\mathcal{S}_1$, performs DL operations during time slot duration τ_1, while the second group, $\mathcal{S}_2$, performs DL operations during time slot duration τ_2. This implies that $\mathcal{S}_1$ performs UL operations in τ_2, and $\mathcal{S}_2$ performs UL operations in τ_1. During DL communication, the UEs harvest energy from a specific proportion of the RF signals received using the PSR method. This harvested power is stored and used to facilitate UL communication. We assume that the channel is reciprocal and remains stable from estimation until data transmission. A simple channel estimation process like [2] is assumed. Both the AP and UEs embed pilot signals in their transmissions. The AP collects the channel estimation results for each UE and use it in the next data transmission for that UE. The AP also estimates its SI channel by analyzing its DL pilot signal. We assume that the energy consumption of pilot signals is negligible due to their minor fraction of frequency resources compared to data signals.

The signal flow of the UEs and AP is described next. Let l and $\hat{l}$ denote the communication phases of the two UE groups in a time slot ($l, \hat{l} \in \{1,2\}$, $\hat{l} = 3 - l$). During the time period τ_l, the signal received from the AP at UE_k of group $\mathcal{S}_l$ at time $t \in \{0 \le t \le \tau_l\}$ is defined as [2], [5], [10]

$$y_{k,l}^{DL}(t) \triangleq \underbrace{\mathbf{h}_{k,l}^H \sum_{j\in\mathcal{S}_l} \mathbf{w}_{j,l} s_j^{DL}(t)}_{\text{AP DL information signals}} + \underbrace{\sum_{j\in\mathcal{S}_{\hat{l}}} \hat{g}_{kj,l}\sqrt{P_{j,l}^{UL}} s_j^{UL}}_{\mathcal{S}_{\hat{l}} \text{ UE UL CI signal}} + z_{k,l}^{DL}(t), \tag{1}$$

where $\mathbf{h}_{k,l} \in \mathbb{C}^{M\times 1}$ is the DL channel and $\hat{g}_{kj,l}$ is the cochannel interference (CI) channel between UE_k and UE_j during τ_l; the $s_j^{DL}(t)$ $(\forall j)$ are the DL signals transmitted from the AP; $\mathbf{w}_{k,l} \in \mathbb{C}^{M\times 1}$ denotes a DL beamformer; $P_{j,l}^{UL}$ $(0 \le P_{j,l}^{UL} \le \hat{Q}_{k,l})$ is the transmit power of UE_j in group $\mathcal{S}_{\hat{l}}$ performing UL operations (with $\hat{Q}_{k,l}$ being the energy harvested at UE_k); and $z_{k,l}^{DL}$ is the noise at UE_k. At UE_k, the DL signal is split into two using the PSR method, where ρ_k denotes the proportion of the signal used for EH, while the rest $(1-\rho_k)$ is used for information decoding.

In the following, we derive the EH model of a G-stage EH rectifier circuit (GSR), as illustrated in Fig. 2. Let $R_{Ld,k}$ (100 kΩ), $R_{At,k}$ (50 Ω), G_k, η_k (1.05) and $V_{T,k}$ (25.86 mV) denote the power management system load, the antenna impedance load, the number of voltage rectifier stages, the ideality factor, and the diode thermal voltage, respectively, for UE_k (the values in parentheses are those used in the evaluation). Let $V_{in,k}$ and $\hat{V}_{out,k}$ be the input voltage and the voltage across a single diode, respectively, of the EH circuit for UE_k. The instantaneous diode current is defined as $i_{dio,k}(t) \triangleq i_{s,k}\left(\exp\left(\frac{V_{in,k}(t)-\hat{V}_{out,k}(t)}{\eta_k V_{T,k}}\right) - 1\right)$ from the Shockley equation, where $i_{s,k}$ is the saturation current. Then, the DC current can be deduced as $i_{dio,k}^{DC} = i_{s,k}\exp\left(\frac{-\hat{V}_{out,k}}{\eta_k V_{T,k}}\right)\exp\left(\frac{f_{LPF}(V_{in,k}(t))}{\eta_k V_{T,k}}\right) - i_{s,k}$, where $f_{LPF}(.)$ represents an ideal low-pass filter describing the function of a capacitor [5], [10]. We assume that $i_{dio,k}^{DC} \approx 0$ due to the low received power and the high impedance of $R_{Ld,k}$ [5]. By applying the Taylor series expansion of an exponential function, truncating at the 4th order and omitting odd-order terms of $V_{in,k}$ (due to no contribution to the DC voltage), we have $\hat{V}_{out,k} \approx \eta_k V_{T,k} \ln\left[1 + \frac{f_{LPF}(V_{in,k}^2(t))}{2\eta_k^2 V_{T,k}^2} + \frac{f_{LPF}(V_{in,k}^4(t))}{24\eta_k^4 V_{T,k}^4}\right]$. Since a single-stage EH rectifier consists of two diodes, the output voltage of the G-stage voltage multiplier is given by $V_{out,k} = 2G_k\hat{V}_{out,k}$. Using $\ln[1+x] \approx x$ and $V_{in,k}(t) = y_k^{ET}(t)\sqrt{R_{At,k}}$ where $y_k^{ET}(t) \triangleq \sqrt{\rho_k} y_{k,l}^{DL}(t)$, one obtains $V_{out,k} \approx \frac{G_k R_{At,k} f_{LPF}(y_k^{ET}(t)^2)}{\eta_k V_{T,k}} + \frac{1}{12}\frac{G_k R_{At,k}^2 f_{LPF}(y_k^{ET}(t)^4)}{\eta_k^3 V_{T,k}^3}$. Finally, the stored output power $\hat{Q}_{k,l}$ is determined as

$$\begin{aligned}\hat{Q}_{k,l} &= V_{out,k}^2 \tau_l/\tau_{\hat{l}} R_{Ld,k} \\ &\approx \frac{\tau_l \rho_k^2 G_k^2 R_{At,k}^2 \sum_{j\in\mathcal{S}_l} |\mathbf{h}_{k,l}^H \mathbf{w}_{j,l}|^2}{4\tau_{\hat{l}} R_{Ld,k}\eta_k^2 V_{T,k}^2}\Big[1 + \frac{\rho_k R_{At,k}}{8\eta_k^2 V_{T,k}^2} \\ &\quad \times \sum_{j\in\mathcal{S}_l} |\mathbf{h}_{k,l}^H \mathbf{w}_{j,l}|^4 + \frac{3\rho_k^2 R_{At,k}^2 \sum_{j\in\mathcal{S}_l} |\mathbf{h}_{k,l}^H \mathbf{w}_{j,l}|^6}{8\eta_k^4 V_{T,k}^4}\Big].\end{aligned} \tag{2}$$

As the output voltage equation of the GSR is more intricate compared to other circuitry, this complexity extends to the following objectives and constraints.

The signal-to-interference-plus-noise ratio (SINR) for UE_k arising from $\sqrt{1-\rho_k} y_{k,l}^{DL}$ is defined as

$$\gamma_{k,l}^{DL} \triangleq \frac{(1-\rho_k)|\mathbf{h}_{k,l}^H \mathbf{w}_{k,l}|^2}{(1-\rho_k)(\sum_{j\in\mathcal{S}_l, j\neq k} |\mathbf{h}_{k,l}^H \mathbf{w}_{j,l}|^2 + \text{CI} + \sigma_{k,l}^2) + \delta_{k,l}^2}, \tag{3}$$

where $\text{CI} = \sum_{j\in\mathcal{S}_{\hat{l}}} |\hat{g}_{kj,l}|^2 P_{j,l}^{UL}$ and $\delta_{k,l}^2$ is the noise power of the information decoding circuit. The UL SINR is derived in the same manner. The signal received at the AP from the UL UEs of $\mathcal{S}_{\hat{l}}$ during τ_l is given as

$$y_l^{UL}(t) = \underbrace{\sum_{k\in\mathcal{S}_{\hat{l}}} \mathbf{g}_{k,l}\sqrt{P_{k,l}^{UL}} s_k^{UL}(t)}_{\mathcal{S}_{\hat{l}} \text{ UE UL information signals}} + \underbrace{\hat{\mathbf{H}}_l \mathbf{s}_l^{DL}(t)}_{\text{RSI at AP}} + z_l^{UL}(t), \tag{4}$$

where $\mathbf{g}_{k,l} \in \mathbb{C}^{M\times 1}$ is the UL channel, $\hat{\mathbf{H}}_l \in \mathbb{C}^{M\times M}$ is the AP SI loop-back channel, meaning that $\hat{\mathbf{H}}_l \mathbf{s}_l^{DL}$ is the

This article has been accepted for publication in IEEE Wireless Communications Letters. This is the author's version which has not been fully edited and content may change prior to final publication. Citation information: DOI 10.1109/LWC.2023.3324984

Algorithm 1 UL and DL sum-rate optimization for a fixed τ_l

1: Initialize: $P^{UL}_{k,\hat{l}}$, $\mathbf{w}_{k,l}$, ρ_k and fixed τ_l, $\forall k$, $\forall l$
2: **repeat**
3: Update each ρ_k, $u_{k,l}$ and $\mathbf{v}_{k,\hat{l}}$ with (10), (9) and (11)
4: Update each $\vartheta^{DL}_{k,\hat{l}}$ and $\vartheta^{UL}_{k,\hat{l}}$ with (8)
5: Update each $P^{UL}_{k,\hat{l}}$ and $\mathbf{w}_{k,l}$ with (12) and (13)
6: Update each $\alpha_{k,1}$ by solving (14) using the BBP
7: **until** system sum-rate convergence

residual SI (RSI) of the AP after imperfect SI cancellation, with $\mathbf{s}^{DL}_l = [s^{DL}_1, \ldots, s^{DL}_j]_{j\in\mathcal{S}_l}$, representing the AP DL information signals, and z^{UL}_l is the noise at the AP. The UL SINR for UE_k in phase l is expressed as

$$\gamma^{UL}_{k,l} = \frac{P^{UL}_{k,l}|\mathbf{v}^H_{k,l}\mathbf{g}_{k,l}|^2}{\sum_{j\in\mathcal{S}_{\bar{l}},j\neq k} P^{UL}_{j,l}|\mathbf{v}^H_{k,l}\mathbf{g}_{j,l}|^2 + \text{RSI} + \sigma^2_l\|\mathbf{v}^H_{k,l}\|^2}, \tag{5}$$

where $\text{RSI} = \hat{\sigma}^2_{\hat{H}}\|\mathbf{v}_{k,l}\|^2\sum_{j\in\mathcal{S}_l}\|\mathbf{w}_{j,l}\|^2$, $\hat{\sigma}^2_{\hat{H}}$ is the RSI noise power and $\mathbf{v}_{k,l}$ is the receive filter at the AP. The total sum rate for the system is calculated as the sum of its UL and DL rates for τ_1 and τ_2. Hence, the FD-SWIPT sum-rate optimization problem is expressed as

$$\begin{aligned}
&\underset{\alpha_{k,l},\tau_l,\mathbf{w}_{k,l},\mathbf{v}_{k,l},P^{UL}_{k,l}}{\text{maximize}} \quad \sum_{k=1}^{K} R^{UD}_k \\
&\text{subject to} \quad \sum_{k=1}^{K}\sum_{l=1}^{2}\|\mathbf{w}_{k,l}\|^2 \le P^{DL}_{0,max}; && \text{(6a)}\\
&\qquad P^{UL}_{k,l} \le \hat{Q}_{k,l},\ \forall k,l; && \text{(6b)}\\
&\qquad 0<\tau_l<1,\ \tau_l+\tau_{\hat{l}}=1; && \text{(6c)}\\
&\qquad 0\le\rho_k\le 1,\ \forall k; && \text{(6d)}\\
&\qquad \alpha_{k,l}+\alpha_{k,\hat{l}}=1, \alpha_{k,l}\in\{0,1\}\ \forall k; && \text{(6e)}\\
&\qquad 1\le|\mathcal{S}_l|<K,\ |\mathcal{S}_l+\mathcal{S}_{\hat{l}}|=K, && \text{(6f)}
\end{aligned} \tag{6}$$

where $R^{UD}_k \triangleq \sum_{l=1}^{2}(\alpha_{k,l}\tau_l\log_2(1+\gamma^{UL}_{k,l})+\alpha_{k,\hat{l}}\tau_{\hat{l}}\log_2(1+\gamma^{DL}_{k,\hat{l}}))$, $P^{DL}_{0,max}$ is the maximum AP transmit power. Constraints (6a) and (6b) are the DL and UL power budgets, respectively. Constraint (6c) is the time resource constraint. Constraint (6d) is the PSR limit. The binary decision variables $\alpha_{k,l}, \alpha_{k,\hat{l}} \in \{0,1\}$ for the assignment of UE_k to either one UE group or the other are constrained by (6e), while (6f) ensures there is at least one UE in each group to activate FD communication.

III. Problem Solution

A. FD Mode AP Operation

Problem (6) is a nonconvex optimization problem, and thus, we develop an iterative algorithm based on the WMMSE approach proposed in [9].

1) Step 1 (Algorithm 1): The process of converting Problem (6) into an equivalent WMMSE problem involves multiple stages. First, the mean squared errors (MSEs) for decoding the UL and DL signals of UE_k are determined as $e^{DL}_{k,l} = |1-\sqrt{(1-\rho_k)}u_{k,l}\mathbf{h}^H_{k,l}\mathbf{w}_{k,l}|^2 + |u_{k,l}|^2\delta^2_{k,l} + |u_{k,l}|^2(1-\rho_k)(\sum_{j\in\mathcal{S}_l,j\neq k}|\mathbf{h}^H_{k,l}\mathbf{w}_{j,l}|^2+\sum_{j\in\mathcal{S}_{\hat{l}}}|\hat{g}_{kj,l}|^2P^{UL}_{j,l}+\sigma^2_{k,l})$ and $e^{UL}_{k,l} = |1-\sqrt{P^{UL}_{k,l}}\mathbf{v}^H_{k,l}\mathbf{g}_{k,l}|^2 + \sum_{j\in\mathcal{S}_{\hat{l}},j\neq k}P^{UL}_{j,l}|\mathbf{v}^H_{k,l}\mathbf{g}_{j,l}|^2 + (\sum_{j\in\mathcal{S}_l}\|\mathbf{w}_{j,l}\|^2\hat{\sigma}^2_{\hat{H}}+\sigma^2_l)\|\mathbf{v}_{k,l}\|^2$, respectively. Then, the DL and UL rates are obtained using the minimum MSE solution. Subsequently, DL and UL MSE weights ($\vartheta^{DL}_{k,l} = 1/e^{DL}_{k,l}$ and $\vartheta^{UL}_{k,l} = 1/e^{UL}_{k,l}$, respectively) are introduced. Finally, based on these weights, the receive filters ($u_{k,l}$ for DL and $\mathbf{v}_{k,l}$ for UL), and the transmit power derivatives, the WMMSE problem is formulated for a fixed τ_l as

$$\underset{\substack{\vartheta^{UL}_{k,l},\vartheta^{DL}_{k,l},u_{k,l},\\ \mathbf{v}_{k,l},\mathbf{w}_{k,l},\rho_k,P^{UL}_{k,l},\alpha_{k,l}}}{\text{minimize}} \quad \Gamma^{UD} \text{ subject to (6a), (6b), (6c) and (6d),} \tag{7}$$

where $\Gamma^{UD} = \sum_{k=1}^{K}\sum_{l=1}^{2}(\vartheta^{DL}_{k,l}e^{DL}_{k,l} - \log\vartheta^{DL}_{k,l}) + \sum_{k=1}^{K}\sum_{l=1}^{2}(\vartheta^{UL}_{k,l}e^{UL}_{k,l} - \log\vartheta^{UL}_{k,l})$. Problem (7) is nonconvex and coupled. Thus we decompose it into single-variable subproblems and conduct alternating optimization, keeping the other variables constant (each subproblem meets the second-order convexity condition [11] with respect to its single problem variable). Thus, $\vartheta^{DL\star}_{k,l}$ and $\vartheta^{UL\star}_{k,l}$ are derived by setting $\partial\Gamma^{UD}_{k,l}/\partial\vartheta^{DL}_{k,l} = 0$ and $\partial\Gamma^{UD}_{k,l}/\partial\vartheta^{UL}_{k,l} = 0$, respectively, and solving for the desired quantity. This results in the following expressions for $\vartheta^{DL\star}_{k,l}$ and $\vartheta^{UL\star}_{k,l}$:

$$\begin{aligned}
\vartheta^{DL}_{k,l} = 1/e^{DL}_{k,l} \approx 1/(1-\sqrt{(1-\rho_k)}u_{k,l}\mathbf{h}^H_{k,l}\mathbf{w}_{k,l}),\\
\vartheta^{UL}_{k,l} = 1/e^{UL}_{k,l} \approx 1/(1-\sqrt{P^{UL}_{k,l}}\mathbf{v}^H_{k,l}\mathbf{g}_{k,l}).
\end{aligned} \tag{8}$$

By defining $\beta = \sum_{j\in\mathcal{S}_l}|\mathbf{h}^H_{k,l}\mathbf{w}_{j,l}|^2 + \sum_{j\in\mathcal{S}_{\hat{l}}}|\hat{g}_{kj,l}|^2P^{UL}_{j,l} + \sigma^2_{k,l}$ and solving $\partial e^{DL}_{k,l}/\partial u_{k,l} = 0$, $u^{\star}_{k,l}$ is deduced as

$$u_{k,l} = \sqrt{(1-\rho_k)}\mathbf{h}^H_{k,l}\mathbf{w}_{k,l}/(\beta(1-\rho_k)+\delta^2_{k,l}). \tag{9}$$

ρ_k is determined from $\partial e^{DL}_{k,l}/\partial\rho_k = 0$ to be

$$\rho_k = 1 - (|\mathbf{h}^H_{k,l}\mathbf{w}_{k,l}|^2/|u_{k,l}|^2\beta^2). \tag{10}$$

Solving $\partial e^{UL}_{k,l}/\partial\mathbf{v}_{k,l} = 0$ for $\mathbf{v}_{k,l}$ yields

$$\mathbf{v}_{k,l} = \Big(\sum_{j\in\mathcal{S}_{\hat{l}}}P^{UL}_{j,l}\mathbf{g}_{j,l}\hat{\mathbf{g}}^H_{j,l} + c\mathbf{I}_M\Big)^{-1}\sqrt{P^{UL}_{k,l}}\mathbf{g}_{k,l}. \tag{11}$$

Based on the constraint (6b), $P^{UL\star}_{k,l}$ is determined from the Lagrangian and Karush–Kuhn–Tucker (KKT) conditions [11] as

$$P^{UL}_{k,l} = \min\Big\{[(\vartheta^{UL}_{k,l}\mathbf{v}^H_{k,l}\mathbf{g}_{k,l})/(B_{k,l}+\lambda^{UL}_k)]^2, \hat{Q}_{k,l}\Big\}, \tag{12}$$

where $\lambda^{UL}_k = \frac{\vartheta^{UL}_{k,l}\mathbf{v}^H_{k,l}\mathbf{g}_{k,l}}{\sum_{l=1}^{2}\sqrt{\hat{Q}_{k,l}}} - \sum_{j\in\mathcal{S}_{\hat{l}}}\vartheta^{DL}_{j,l}(1-\rho_j)|u_{j,l}|^2|\hat{g}_{kj,l}|^2 - \sum_{j\in\mathcal{S}_{\hat{l}}}\vartheta^{UL}_{j,l}|\mathbf{v}^H_{j,l}\mathbf{g}_{k,l}|^2$ and $B_{k,l} = \sum_{j\in\mathcal{S}_{\hat{l}}}\vartheta^{DL}_{j,l}|u_{j,l}|^2|\hat{g}_{kj,l}|^2(1-\rho_j) + \sum_{j\in\mathcal{S}_{\hat{l}}}\vartheta^{UL}_{j,l}|\mathbf{v}^H_{j,l}\mathbf{g}_{k,l}|^2$. Combining the WMMSE problem with constraint (6a) and solving for $\mathbf{w}_{k,l}$ from the Lagrangian and KKT conditions yields

$$\mathbf{w}_{k,l} \approx \mathbf{A}^{-1}(\sqrt{1-\rho_k}\mathbf{h}_{k,l}u_{k,l}\vartheta^{DL}_{k,l}), \tag{13}$$

where $\mathbf{A} = \sum_{j\in\mathcal{S}_l}\vartheta^{DL}_{j,l}|u_{j,l}|^2\mathbf{h}_{j,l}\mathbf{h}^H_{j,l}(1-\rho_j) + \lambda^{DL}\mathbf{I}_M + \sum_{j\in\mathcal{S}_l}\vartheta^{UL}_{j,l}\|\mathbf{V}_{j,l}\|^2\hat{\sigma}^2_{\hat{H}}\mathbf{I}_M$ and $\lambda^{DL} \approx \sum_{k=1}^{K}\sum_{l=1}^{2}(1/P_{0,max}) \times [\vartheta^{UL}_{k,l}\sigma^2_l|\mathbf{V}_{k,l}|^2 + \vartheta^{DL}_{k,l}|u_{k,l}|^2(\delta^2_{k,l}+\sigma^2_{k,l}(1-\rho_k))]$.

The UE grouping problem is defined as

$$\underset{\alpha_{k,l}}{\text{maximize}} \sum_{k=1}^{K} R_k^{UD} \text{ subject to (6e) and (6f),} \tag{14}$$

which is a mixed-integer linear programming (MILP) problem and can be solved using a generic MILP solver such as the branch-and-bound procedure (BBP) [2].

2) Step 2 (Algorithm 2): The time allocation problem is defined as

$$\underset{\tau_l}{\text{maximize}} \sum_{k=1}^{K} R_k^{UD} \text{ subject to (6b), (6c) and (6d).} \tag{15}$$

Therefore, the optimal τ_l is determined using an iterative line search method after the values of all other problem variables have been found in Step 1.

B. Implementation, Overhead, and Complexity Reduction

Algorithms 1 and 2 are implemented centrally at the AP since the AP collects the channel statistics associated with the UEs. The AP determines the optimal variables and transmits $\{\rho_k\}_{k=1}^K$ and $\{P_{k,l}^{UL}\}_{k=1}^K$ to the UEs. The Big O computational complexities for executing Algorithms 1 and 2 are $O(I_I[K^2 + 2^{10}K^{10}])$ and $O(I_O[I_I[K^2 + 2^{10}K^{10}] + K + \log(1/\epsilon)])$, respectively, where I_I, I_O, and ϵ represent the computations for the iteration of Algorithm 1, the iteration of Algorithm 2 and the convergence criterion, respectively. The total number of arithmetic calculations for the variables $\{u_{k,l}\}_{k=1,l=1}^{K,2}$, $\{\mathbf{v}_{k,l}\}_{k=1,l=1}^{K,2}$, $\{\vartheta_{k,l}^{UL}\}_{k=1,l=1}^{K,2}$, $\{\vartheta_{k,l}^{DL}\}_{k=1,l=1}^{K,2}$, $\{P_{k,l}^{UL}\}_{k=1,l=1}^{K,2}$, $\{\mathbf{w}_{k,l}\}_{k=1,l=1}^{K,2}$, $\{\alpha_{k,l}\}_{k=1,l=1}^{K,2}$ and $\{\lambda_{k,l}^{UL}\}_{k=1,l=1}^{K,2}$ and the sum-rate (UL and DL) convergence calculation is $2^{10}K^{10}$. The number of arithmetic calculations for $\{\rho_k\}_{k=1}^K$ is K. The number of bits for transmitting $\{\rho_k\}_{k=1}^K$ and $\{P_{k,l}^{UL}\}_{k=1}^K$ to the UEs is $K(i_0 + 2B) + F$, where i_0, B and F are the numbers of UE index bits, real-number bits (for ρ_k or $P_{k,l}^{UL}$) and information bits, respectively.

In order to mitigate the complexity inherent in Algorithm 1, we introduce three variants. The first two employ equal DL power allocation and fixed PSR, utilizing (a) zero-forcing (ZF) and (b) maximum ratio combining (MRC) for the AP beamformers. Both variants offer reduced computational complexity as $O(I_O[I_I[K^2 + 2^7K^7] + 3K + \log(1/\epsilon)])$. The third variant adopts a staggered (Stg) update strategy, where a problem variable is updated every n_{stg} iterations if the gap between its previous and current values is smaller than e_{stg}. This approach reduces computational demands, operating at $O(I_O[I_I[K^2 + 2^xK^x] + K + \log(1/\epsilon)])$, with $x(\leq 10)$ denoting the number of variables updated per iteration.

IV. Numerical Evaluation and Discussion

Simulation results for FD-SWIPT with different EH models and optimization schemes are presented in this section, where we denote the proposed resource allocation scheme by Opt. As a benchmark, we also evaluate the corresponding HD-SWIPT model (i.e., for HD AP) in which the RSI and CI components are not present. Hence, $\hat{\sigma}_{\hat{\mathbf{H}}}^2 \|\mathbf{v}_{k,\hat{l}}\|^2 \sum_{j\in\mathcal{S}_{\hat{l}}} \|\mathbf{w}_{j,\hat{l}}\|^2$ and $\sum_{j\in\mathcal{S}_{\hat{l}}} \hat{g}_{kj,l}\sqrt{P_{j,l}^{UL}}$ are removed from the SINR equations, and only (9), (10), (11), (12) and (13) are used.

The simulated topology consists of UEs randomly distributed around an AP within a radius of 10 meters. A Rician fading channel model is considered, which is defined as $\sqrt{A_0(c/4\pi f d_{i,j})^\alpha G_t G_r}(\sqrt{\kappa/(\kappa+1)}\hat{\mathbf{h}}_{k,l} + \sqrt{1/(\kappa+1)}\tilde{\mathbf{h}}_{k,l})$, where A_0, c, f, α and κ are the signal attenuation (10 dB), the speed of light (3×10^8 m/s), the carrier frequency (2.4 GHz), the path-loss exponent (2.5), and Rician factor (3), respectively. The time domain correlation is considered with a Doppler shift of 5 Hz and a spatial correlation of 0.95. G_t and G_r are the antenna gains of the AP and UEs, respectively, both set to 6 dBi. $d_{\{i,j\}}$ is the internode distance. $\hat{\mathbf{h}}_{k,l}$ and $\tilde{\mathbf{h}}_{k,l}$ are the line-of-sight (LOS) and non-LOS small-scale fading components. We consider $\sigma_l^2 = \sigma_{k,l}^2 = -80$ dBm, $\delta_{k,l}^2 = -80$ dBm, $\hat{\sigma}_{\hat{\mathbf{H}}}^2 = -120$ dBm, and $M = K = 4$. For Stg, we set $n_{stg} = 2$ and $e_{stg} = 0.01$. Unless specified otherwise, the GSR EH model is used and the number of rectifier stages G of the GSR model is set to four. The circuit model parameters are given in Section II. We used Matlab's MILP solver for UE grouping.

A. Performance of the Proposed Scheme

The convergence behavior of the algorithm under two different variable initialization scenarios is presented in Fig. 3, including the brute-force search (BFS) method, where each variable undergoes BFS updates within the framework of Algorithm 1. Notably, BFS exhibits a higher computational complexity, scaling as $O(I_O[I_I[K^2 + (2K) + 2K + K\log(1/\epsilon))]^5 + K^2 + \log(1/\epsilon))]$. Opt, Stg and BFS converge to similar sum-rate values. However, BFS achieves convergence in fewer iterations by employing optimal variable values in each iteration. Stg, though distributing computational load across iterations, requires almost twice as many iterations as Opt for convergence.

Fig. 4 presents an analysis of Opt and random (Rand) schemes for UE grouping using different EH models: the proposed GSR, simple rectifier (SR) [5], nonlinear threshold (NL) [2], and linear (L) [3] models. Opt consistently outperforms Rand across all EH models, underscoring the crucial role of UE grouping. In particular, at $\hat{P}_{0,max}^{DL} = 30$ dB, GSR Opt outperforms GSR Rand by 6 bps/Hz, while SR Opt shows a 5 bps/Hz advantage over SR Rand, and NL/L Opt surpasses NL/L Rand by 3 bps/Hz.

The UL and DL sum rates of the proposed resource allocation scheme are plotted against the signal-to-noise ratio (SNR, $\hat{P}_{0,max}^{DL} = P_{0,max}^{DL}/\sigma$) in Fig. 5. Opt yields higher data rates than the ZF and MRC benchmarks for both FD and HD modes. Opt exhibits a reliable gain of 15 and 18 bps/Hz for ZF and MRC in the FD- and HD-SWIPT systems, respectively, highlighting the tradeoff between system performance and complexity. HD-SWIPT becomes superior to FD-SWIPT at higher $\hat{P}_{0,max}^{DL}$ due to the excessive RSI in the FD mode.

B. Performance of the EH Models

Fig. 6 illustrates that, in most cases, Opt and Stg yield higher harvested power compared to ZF and MRC. As the

This article has been accepted for publication in IEEE Wireless Communications Letters. This is the author's version which has not been fully edited and content may change prior to final publication. Citation information: DOI 10.1109/LWC.2023.3324984

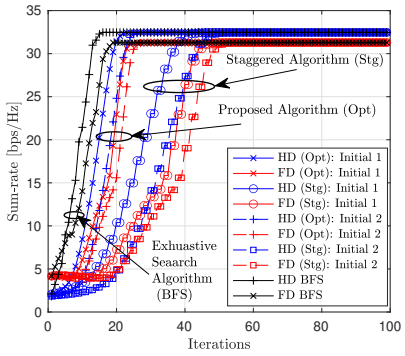

Fig. 3. Sum rate over iterations.

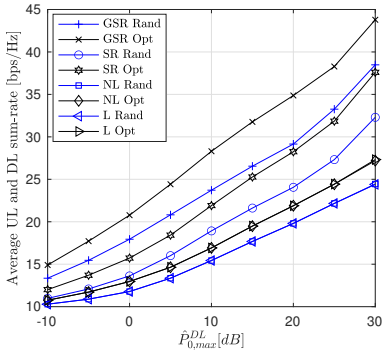

Fig. 4. Sum rates of FD-SWIPT with different UE groupings.

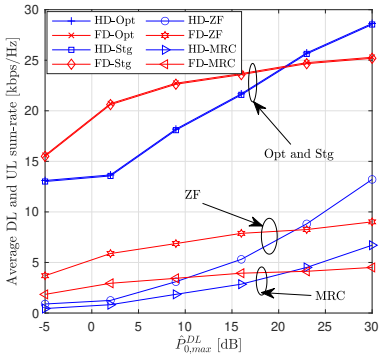

Fig. 5. Average network sum rate vs. $\hat{P}^{DL}_{0,max}$.

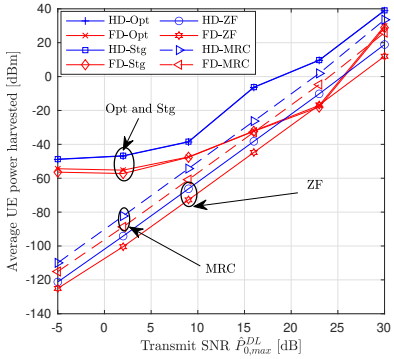

Fig. 6. Average UE power harvested vs. $\hat{P}^{DL}_{0,max}$.

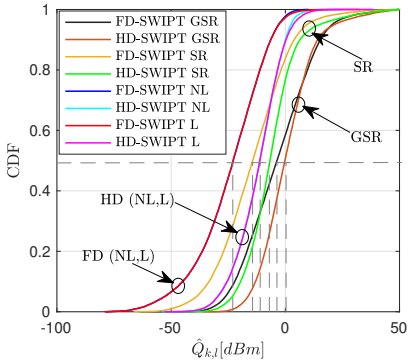

Fig. 7. CDF of $\hat{Q}_{k,l}$.

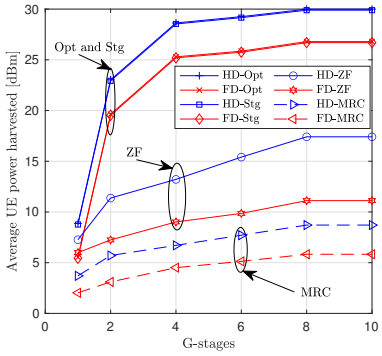

Fig. 8. Average UE power harvested vs. the number of stages G.

transmit SNR increases, however, the gain of Opt decreases since adaptive power allocation becomes less effective in optimizing performance when the receive power strength reaches sufficiently high levels. The HD-SWIPT system harvests more power than the FD-SWIPT system due to the necessity of effective SI suppression in determining the DL beamformer $\mathbf{w}_{k,l}$ for the FD-SWIPT system, which adversely affects the power harvesting performance. The cumulative distribution functions (CDFs) of the power harvested by the UEs are given in Fig. 7, showing that the GSR model results in the highest harvested power at all points along the curves. It is shown in Fig. 8 ($\hat{P}^{DL}_{0,max}$ = 30 dB) that the harvested power under the GSR model increases with increasing G and plateau at $G \geq 8$ for both the FD and HD modes.

V. Conclusion

We addressed radio resource allocation in an FD-SWIPT system, deriving an advanced multistage rectifier circuit EH model. We developed an iterative algorithm using the WMMSE approach to optimize transmit and receive beamformers, UE grouping, and slot durations for DL and UL sum-rate maximization.

References

[1] J. I. Choi, M. Jain, K. Srinivasan, P. Levis, and S. Katti, "Achieving single channel, full duplex wireless communication," in *Proc. ACM MobiCom*, 2010.

[2] D. K. P. Asiedu, S. Mahama, C. Song, D. Kim, and K.-J. Lee, "Beamforming and resource allocation for multi-user full-duplex wireless powered communications in IoT networks," *IEEE Internet of Things J.*, May 2020.

[3] Z. Wen, Z. Guo, N. C. Beaulieu, and X. Liu, "Robust beamforming design for multi-user MISO full-duplex SWIPT system with channel state information uncertainty," *IEEE Trans. Veh. Technol.*, vol. 68, no. 2, pp. 1942–1947, Dec. 2018.

[4] L. Zheng, D. Liu, Z. Wen, and J. Zou, "Robust beamforming for multi-user MISO full-duplex SWIPT system under non-linear energy harvesting model," *IEEE Access*, vol. 9, pp. 14 387–14 397, Jan. 2021.

[5] S. Shen and B. Clerckx, "Beamforming optimization for MIMO wireless power transfer with nonlinear energy harvesting: RF combining versus DC combining," *IEEE Trans. Wireless Commun.*, vol. 20, no. 1, pp. 199–213, 2020.

[6] E. Boshkovska, D. W. K. Ng, N. Zlatanov, and R. Schober, "Practical non-linear energy harvesting model and resource allocation for SWIPT systems," *IEEE Commun. Let.*, vol. 19, no. 12, pp. 2082–2085, Sep. 2015.

[7] S. García-Moreno, M. A. Gurrola-Navarro, C. A. Bonilla-Barragán, and I. Mejía, "Design method for RF energy harvesting rectifiers," *IEEE Trans. Circuits Sys. II: Express Briefs*, vol. 67, no. 11, pp. 2727–2731, Jan. 2020.

[8] I. Budhiraja, N. Kumar, S. Tyagi, S. Tanwar, and M. Guizani, "SWIPT-enabled D2D communication underlaying NOMA-based cellular networks in imperfect CSI," *IEEE Trans. Veh. Technol.*, vol. 70, no. 1, pp. 692–699, Jan. 2021.

[9] S. S. Christensen, R. Agarwal, E. De Carvalho, and J. M. Cioffi, "Weighted sum-rate maximization using weighted MMSE for MIMO-BC beamforming design," *IEEE Trans. Wireless Commun.*, vol. 7, no. 12, pp. 4792–4799, Dec. 2008.

[10] Y. Huang and B. Clerckx, "Waveform design for wireless power transfer with limited feedback," *IEEE Trans. Wireless Commun.*, vol. 17, no. 1, pp. 415–429, Nov. 2017.

[11] S. Boyd and L. Vandenberghe, *Convex Optimization*. Cambridge university press, 2004.